

# ON THE EIGENFREQUENCY OPTIMIZATION OF EULER-BERNOULLI BEAMS WITH NONLOCAL DAMPING PATCHES

Ligia MUNTEANU<sup>1</sup>, Veturia CHIROIU<sup>1</sup>, Dan DUMITRIU<sup>1</sup>, Daniel BALDOVIN<sup>1</sup>,  
Călin CHIROIU<sup>2</sup>

The paper discusses the bending of Euler-Bernoulli beams with external nonlocal damping patches. Unlike ordinary local damping models, the nonlocal damping force is modeled as a weighted average of the velocity field over the spatial domain, determined by a kernel function based on distance measures. The performance with respect to eigenvalues is discussed in order to avoid resonance. The optimization is performed by determining the location of patches from maximizing eigenvalues or gap between them.

## 1. INTRODUCTION

The ability of tailoring the best behavior of beams at vibrations consists in a qualitative and quantitative understanding of the damping properties. One way to manipulate the eigenfrequencies of the beams is to vary its damping capacity. Currently, it is impossible to obtain an optimal solution by maximizing eigenfrequencies or gaps between them, or by minimizing the possibility of internal resonance (Abrete [1], Pedersen [2-4]) for ordinary local damping models. The nonlocal theory describes long-range interactions among the particles, the stress at a location being determined by interatomic interactions in the neighbors around that location. In this theory, the damping force is obtained as a weighted average of the velocity field over the spatial domain, by a kernel function based on distance measures. The deformations at one position produce forces and moments at other points in the structure (Eringen and Edelen [5], Polizzotto [6]). The interest in the subject has resulted in a large number of papers which describe nonlocal damping models based on viscoelasticity (Ahmadi [7]), on the harmonic waves motion in Voigt–Kevin and Maxwell media (Nowinski [8]), or on composites with the internal damping torque (Russell [9], Ghoneim [10]), and so on. Lei, Friswell and Adhikari [11] have developed a nonlocal damping model including time and spatial hysteresis effects for Euler-Bernoulli beams and Kirchoff plates.

The starting point of the Lei, Friswell and Adhikari theory is the damping force which depends at a given point on the past history of a velocity field over a

---

<sup>1</sup> Institute of Solid Mechanics, Romanian Academy, Ctin Mille 15, 010141 Bucharest

<sup>2</sup> Fast Informatica, Torino 10138

Corresponding author e-mail: ligia\_munteanu@hotmail.com

certain domain, through a kernel function. In this paper we apply the Lei, Friswell and Adhikari theory to analyze the dynamic characteristics of the Euler-Bernoulli beams with external nonlocal damping patches. The shear and rotational forces are negligible for this model. The positions of the patches are determined from optimality criteria of maximizing eigenvalues or gap between them in order to avoid resonance. The eigenvalues and optimization problems are solved by the genetic algorithm.

## 2. THE MODEL OF NONLOCAL DAMPING

The governing equation of motion for a 1D linear damped continuous dynamic system may be expressed as (Lei, Friswell and Adhikari [11]).

$$Lu(x,t) = 0, \quad x \in \Omega, \quad t \in [0, T], \quad (2.1)$$

where  $u(x,t)$  is the displacement vector,  $x$  is the spatial variable,  $t$  is time, and  $L$  is the nonlocal operator defined by

$$Lu(x,t) = \rho(x) \frac{\partial^2}{\partial t^2} u(x,t) + M \frac{\partial}{\partial t} u(x,t), \quad (2.2)$$

where  $\rho(x)$  is the distributed mass density. The operator  $M$  is defined as

$$M \frac{\partial}{\partial t} u(x,t) = \int_{\Omega_0}^t C(x, \xi, t - \tau) \frac{\partial}{\partial t} u(\xi, \tau) d\tau d\xi, \quad (2.3)$$

with  $C(x, \xi, t - \tau)$  the kernel function for external damping which is only dependent on the displacement. Equation (2.1) is subjected to the initial conditions

$$u(x,0) = u_0(x), \quad \frac{\partial}{\partial t} u(x,t) \Big|_{t=0} = v_0(x), \quad (2.4a)$$

where  $u_0(x)$  and  $v_0(x)$  are the initial displacement and velocity. The boundary conditions are given by

$$u(x,t) = \bar{g}_1(x,t) \text{ for } x \in \Gamma_1, \quad \frac{\partial}{\partial x} u(x,t) = \bar{g}_2(x,t) \text{ for } x \in \Gamma_2, \quad (2.4b)$$

where  $\Gamma_1$  and  $\Gamma_2$  are the boundary domains, and  $\bar{g}_1(x,t)$  and  $\bar{g}_2(x,t)$  are known functions at the boundary. If the damping kernel functions are assumed to be separable in space and time, we can write  $C(x, \xi, t - \tau)$  in a general form

$$C(x, \xi, t - \tau) = H(x)c(x - \xi)g(t - \tau). \quad (2.5)$$

The expression (2.5) represents the general form of nonlocal viscoelastic damping model. The function  $H(x)$  denotes the presence of nonlocal damping. We have  $H(x) = H_0$  (constant) if  $x$  is within the patch, and  $H(x) = 0$  otherwise. A

particular case of (2.5) is the nonlocal viscous damping (or spatial hysteresis), where the kernel function is given by a delta function in time. In this case, the force depends only on the instantaneous value of the velocity or strain rate

$$g(t - \tau) = \delta(t - \tau), \quad (2.6)$$

but depends on the spatial distribution of the velocities

$$C(x, \xi, t - \tau) = H(x)c(x - \xi)\delta(t - \tau). \quad (2.7)$$

In (2.7), velocities at different locations within a certain domain can affect the damping force at a given point. This spatial hysteresis that describes the damping mechanism for quasi-isotropic composite beams is similar to the damping model proposed by Banks and Inman [12], Banks *et al.* [13] and Sorrentino *et al.* [14]. The spatial kernel function,  $c(x - \xi)$  is normalized to satisfy the condition

$$\int_{-\infty}^{\infty} c(x)dx = 1, \quad (2.8)$$

and can be choose as an exponential decay or respectively, an error function

$$\begin{aligned} c(x - \xi) &= \frac{\alpha}{2} \exp(-\alpha |x - \xi|), \\ c(x - \xi) &= \frac{\alpha}{\sqrt{2\pi}} \exp\left(-\frac{1}{2}\alpha^2(x - \xi)^2\right). \end{aligned} \quad (2.9a)$$

Here  $\alpha$  is a characteristic parameter of the damping material. For  $\alpha \rightarrow \infty$  it results  $c(x - \xi) \rightarrow 0$ . Another form of  $c(x - \xi)$  may be taken as the hat respectively, the triangular shapes

$$\begin{aligned} c(x - \xi) &= \frac{1}{l_0} \text{ for } |x - \xi| \leq \frac{l_0}{2}, \text{ and } 0 \text{ otherwise,} \\ c(x - \xi) &= \frac{1}{l_0} \left(1 - \frac{|x - \xi|}{l_0}\right) \text{ for } |x - \xi| \leq l_0, \text{ and } 0 \text{ otherwise,} \end{aligned} \quad (2.9b)$$

where  $l_0$  is the influence distance parameter. It results  $c(x - \xi) \rightarrow 0$  for  $|x - \xi| > l_0$ . Another form for  $c(x - \xi)$  may be the Dirac delta function  $\delta(x - \xi)$ , which reflects the reacting character of the damping force

$$c(x - \xi) = \delta(x - \xi). \quad (2.10)$$

In the case of a reacting damping force (2.10), there are two cases of  $C(x, \xi, t - \tau)$  from (2.5):

(i) viscoelastic damping (or time hysteresis) with the kernel depending on the past time histories

$$C(x, \xi, t - \tau) = H(x)\delta(x - \xi)g(t - \tau); \quad (2.11)$$

(ii) viscous damping with the force depending only on the instantaneous value of the velocity or strain rate

$$C(x, \xi, t - \tau) = H(x) \delta(x - \xi) \delta(t - \tau). \quad (2.12)$$

The model (2.12) represents the well-known viscous damping model. For the kernel function concerned to time  $g(t - \tau)$ , we consider

$$g(t - \tau) = g_0 \mu \exp(-\mu(t - \tau)), \quad (2.13)$$

with  $\mu$  the relaxation constant of the viscoelastic constant for external damping kernel and  $g_0$  a constant.

### 3. THE NONLOCAL DAMPED BEAM

Consider a beam of length  $L$ , in which a number  $k_p$  of external nonlocal damping muffled patches of thickness  $h_p$  are attached at  $(x_1, x_1 + \Delta x_1)$ ,  $(x_2, x_2 + \Delta x_2)$ , ...,  $(x_k, x_k + \Delta x_k)$ ,  $x_2 \geq x_1 + \Delta x_1$ ,  $x_i \geq x_{i-1} + \Delta x_{i-1}$ ,  $i = 2, \dots, k$ , (Lei, Friswell and Adhikari [11]) as shown in Fig. 3.1.

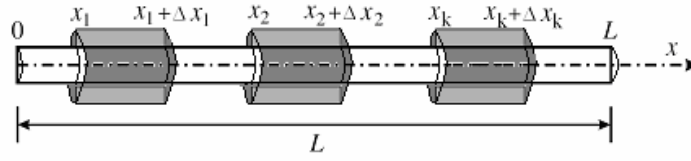


Fig. 3.1 – The beam with nonlocal damping muffled patches.

The design parameters are the number  $k_p$  of patches, coordinates  $x_j$ , and lengths of patches  $\Delta x_j$ ,  $j = 1, 2, \dots, k_p$ , under the conditions  $x_2 \geq x_1 + \Delta x_1$ ,  $x_i \geq x_{i-1} + \Delta x_{i-1}$ ,  $i = 2, \dots, k_p$ . Since the number of parameters is high, the possible different reduction of the parameter number is versatile. In the forward problem these parameters are known. The equation of motion for the beam is

$$\frac{\partial}{\partial x^2} \left( EI(x) \frac{\partial^2 w(x, t)}{\partial x^2} \right) + \rho A(x) \frac{\partial^2 w(x, t)}{\partial t^2} + \Upsilon = 0, \quad (3.1)$$

where  $EI(x)$  is the bending stiffness ( $E$  the Young's modulus of elasticity and  $I(x)$  the moment of inertia),  $\rho A(x)$  is the mass per unit length ( $\rho$  the density and  $A(x)$  the cross section area),  $w(x, t)$  is the transverse displacement. The third term represents the nonlocal external damping defined over the spatial subdomains  $(x_i, x_i + \Delta x_i)$ ,  $i = 1, 2, \dots, k$ , as

$$\Upsilon = \sum_{i=1}^k \int_{x_i}^{x_i + \Delta x_i} \int_{-\infty}^t C(x, \xi, t - \tau) \frac{\partial w(\xi, \tau)}{\partial t} d\tau d\xi. \quad (3.2)$$

The damping kernel is defined by (2.5) with the particular case of the nonlocal viscous damping (or spatial hysteresis), with  $C(x, \xi, t - \tau)$  given by (2.7). We choose for  $c(x - \xi)$  the exponential decay and the error function given by (2.9a), hat form and the triangular shapes given by (2.9b) and the Dirac delta function  $\delta(x - \xi)$ , with both forms for  $C(x, \xi, t - \tau)$  namely (2.11) and (2.12). The initial conditions (2.4a) are written as

$$w(x, 0) = w_0(x), \quad \frac{\partial}{\partial t} w(x, t) \Big|_{t=0} = v_0(x). \quad (3.3)$$

The boundary conditions (2.4b) are written for a clamped beam

$$w(x, t) = 0, \quad \frac{\partial w(x, t)}{\partial x} = 0, \quad \text{for } x = 0, \quad x = L, \quad (3.4a)$$

for a simple supported beam

$$w(x, t) = 0, \quad \frac{\partial^2 w(x, t)}{\partial x^2} = 0, \quad \text{for } x = 0, \quad x = L, \quad (3.4b)$$

and for a free end beam

$$\frac{\partial^2 w(x, t)}{\partial x^2} = 0, \quad \frac{\partial}{\partial x} \left[ EI(x) \frac{\partial^2 w(x, t)}{\partial x^2} \right] = 0, \quad \text{for } x = 0, \quad x = L. \quad (3.4c)$$

The eigenfrequency problem (3.1)-(3.4) is characterised by the integro-differential equation (3.1), which can be analytically solved by using the cnoidal method (Munteanu and Donescu [15], Chiroiu and Chiroiu [16], Osborne [17]).

The general solutions of (3.1) must be found under the form of a sum of cnoidal functions

$$w(x, t) = \sum_{j=1}^N A_j \text{cn}^2(\eta | m_j), \quad \eta = kx - \omega t + \varphi, \quad (3.5)$$

where  $N$  is the number of cnoidal functions (Jacobian elliptic functions) considered in the series depending on the accuracy required,  $A_j$  are unknown constants,  $k$  is the wave number, the  $\omega$  is the frequency and the  $\varphi$  is the phase. The Jacobian elliptic function  $\text{cn}(\eta | m) = \text{cn} \eta$  can be defined with respect to the integral

$$\eta = \int_0^\varphi \frac{d\theta}{\sqrt{1 - m \sin^2 \theta}}, \quad 0 \leq m \leq 1,$$

thus

$$\operatorname{sn}\eta = \sin\varphi, \quad \operatorname{cn}\eta = \cos\varphi, \quad \operatorname{dn}\eta = \sqrt{1 - m\sin^2\varphi}.$$

For  $m=0$  it is obtained  $\operatorname{sn}\eta = \sin\eta$ ,  $\operatorname{cn}\eta = \cos\eta$ ,  $\operatorname{dn}\eta = 1$ , and for  $m=1$ ,  $\operatorname{sn}\eta = \tanh\eta$ ,  $\operatorname{cn}\eta = \operatorname{sech}\eta$ ,  $\operatorname{dn}\eta = \operatorname{sech}\eta$ . By denoting  $\eta|m_j = \eta_j$  and introducing (3.5) into (3.1) we have

$$\frac{\partial}{\partial x^2} \left( EI(x) \frac{\partial^2}{\partial x^2} \left( \sum_{j=1}^N A_j \operatorname{cn}^2 \eta_j \right) \right) + \rho A(x) \frac{\partial^2}{\partial t^2} \left( \sum_{j=1}^N A_j \operatorname{cn}^2 \eta_j \right) + \Upsilon = 0, \quad (3.6)$$

with

$$\Upsilon = \sum_{i=1}^k \int_{x_i}^{x_i + \Delta x_i} \int_{-\infty}^t C(x, \xi, t - \tau) \frac{\partial}{\partial t} \left( \sum_{j=1}^N A_j \operatorname{cn}^2 \zeta_j \right) d\tau d\xi, \quad \zeta_j = k_j \xi - \omega_j \tau + \varphi_j. \quad (3.7)$$

The advantage of the cnoidal method consists in the easier mode to choose the constants  $A_j$ ,  $j=1, 2, \dots, N$  by imposing the boundary conditions (3.4) to be satisfied. The eigenvalues are finding by solving the eigenvalue problem (3.6), (3.7) and (3.3), (3.4).

Let us suppose that the bar is circular with varying diameter  $d(x) = d_0 \left( 2 - a \frac{x}{L} \right) = d_0 (2 - bx)$ . For  $b=0$  the rod will have a uniform diameter  $2d_0$ . The area of cross section is  $A(x) = \frac{\pi d^2(x)}{4} = A_0 (2 - bx)^2$  with  $A_0 = \frac{\pi d_0^2}{4}$ , and the moment of inertia is  $I(x) = \frac{\pi d^4(x)}{64} = I_0 (2 - bx)^4$  with  $I_0 = \frac{\pi d_0^4}{64}$ .

#### 4. THE EIGENVALUE FORWARD PROBLEM

Upon some algebra and taking account on formulae

$$\begin{aligned} \frac{\partial^2}{\partial x^2} \left( \sum_{j=1}^N A_j \operatorname{cn}^2 \eta_j \right) &= 2k^2 \sum_{j=1}^N (1 - m_j + A_j (3m_j - 2) \operatorname{cn}^2 \eta_j - A_j m_j \operatorname{cn}^4 \eta_j), \\ \frac{\partial^2}{\partial t^2} \left( \sum_{j=1}^N A_j \operatorname{cn}^2 \eta_j \right) &= 2\omega^2 \sum_{j=1}^N (1 - m_j + A_j (3m_j - 2) \operatorname{cn}^2 \eta_j - A_j m_j \operatorname{cn}^4 \eta_j), \\ \frac{\partial}{\partial t} \left( \sum_{j=1}^N A_j \operatorname{cn}^2 \eta_j \right) &= 2\omega \sum_{j=1}^N A_j \operatorname{cn} \eta_j \operatorname{sn} \eta_j \operatorname{dn} \eta_j, \end{aligned}$$

$$\text{cn}^2\eta_j + \text{sn}^2\eta_j = 1, \text{dn}^2\eta_j + m\text{sn}^2\eta_j = 1,$$

the eigenvalue problem is reduced to the equation

$$\sum_{j=1}^N (P_j + \rho\omega^2 Q_j + \omega R_j + Y_j) = 0, \quad (4.1)$$

where  $P, Q, R$  are polynomials in  $\text{cn}$ ,  $\text{sn}$  and  $\text{dn}$ , and

$$Y_j = 2\omega A_j \sum_{i=1}^k \int_{x_i}^{x_i + \Delta x_i} \int_{-\infty}^t C(x, \xi, t - \tau) (\text{cn}\eta_j \text{sn}\eta_j \text{dn}\eta_j) d\tau d\xi, \quad (4.2)$$

$$\eta_j = \eta | m_j = k\xi - \omega\tau + \varphi.$$

By equating the terms with the same power in  $\text{cn}$ ,  $\text{sn}$  and  $\text{dn}$ , a number of  $K$  equations are obtained from (4.1)

$$\begin{aligned} \lambda_1(A_j, m_j, k, \varphi) &= \omega_1, \\ \lambda_2(A_j, m_j, k, \varphi) &= \omega_2, \\ \lambda_K(A_j, m_j, k, \varphi) &= \omega_K. \end{aligned} \quad (4.3)$$

The number of unknowns  $p_M = \{A_j, m_j, k, \varphi, \omega, j = 1, 2, \dots, k_p\}$ ,  $M = 2k_p + 3$ , is obviously greater than the number of equations  $K < M$ . A less restrictive approach for the solving of (4.3) is to form the residuals functions  $r_K$

$$\lambda_l(A_j, m_j, k, \varphi) - \omega_l = r_l, \quad l = 1, 2, \dots, K. \quad (4.4)$$

The problem becomes one of minimizing the combined residuals to calculate accurate values for  $p_M$ . To solve the eigenvalue problem, a nonlinear least-squares algorithm is proposed. The objective function is defined by

$$\mathfrak{J}(p_j) = K^{-1} \sum_{l=1}^K r_l^2(p_j) + (4N_1)^{-1} \sum_{n=1}^{N_1} \sum_{i=1}^2 \delta_{in}^2(p_j) + \sum_{j=1}^6 \delta_j^2(p_j), \quad (4.3)$$

where  $\delta_{in}(p_j)$ ,  $i = 1, 2$ ,  $n = 1, 2, \dots, N_1$ , are two control indicators of the verification of initial conditions (3.3) in the points  $x_n$ ,  $n = 1, 2, \dots, N_1$

$$\delta_{1n} = w(x_n, 0) - w_0(x_n), \quad \delta_{2n} = \frac{\partial}{\partial t} w(x_n, 0) - v_0(x_n). \quad (4.4)$$

The boundary conditions (3.4) have associated also the control indicators to verify the conditions for a clamped beam

$$\delta_3 = w(0,0), \delta_4 = w(L,0), \delta_5 = \frac{\partial w(0,0)}{\partial x}, \delta_6 = \frac{\partial w(L,0)}{\partial x}, \quad (4.4a)$$

for a simple supported beam

$$\delta_3 = w(0,0), \delta_4 = w(L,0), \delta_5 = \frac{\partial^2 w(0,0)}{\partial x^2}, \delta_6 = \frac{\partial^2 w(L,0)}{\partial x^2}. \quad (4.4b)$$

or a free end beam

$$\begin{aligned} \delta_3 &= \frac{\partial^2 w(0,0)}{\partial x^2}, \delta_4 = \frac{\partial^2 w(L,0)}{\partial x^2}, \delta_5 = \frac{\partial}{\partial x} \left[ EI(0) \frac{\partial^2 w(0,0)}{\partial x^2} \right], \\ \delta_6 &= \frac{\partial}{\partial x} \left[ EI(L) \frac{\partial^2 w(L,0)}{\partial x^2} \right]. \end{aligned} \quad (4.4c)$$

The unknowns  $p_M = \{A_j, m_j, k, \varphi, \omega, j=1, 2, \dots, k_p\}$ ,  $M = 2k_p + 3$ , are determined by using a genetic algorithm. The genetic algorithm assures an iteration scheme that guarantees a closer correspondence of required conditions at each iteration.

We show that the knowledge of the geometry and properties of the beam is sufficient to evaluate the eigenvalues.

## 5. NUMERICAL EXAMPLES

*Example 5.1.* Let us consider a simply supported aluminum beam of length  $L = 2$  m, with constant diameter  $d = 0.005$  m, the Young's modulus  $E = 70$  GPa and the mass density  $\rho = 2700$  kg/m<sup>3</sup>, with a single patch  $k_p = 1$ ,  $x_1 = 0.2$  m and  $\Delta x_1 = 0.2$  m, and thickness  $h_p = 0.003$  m. We consider two cases: the nonlocal viscoelastic damping (or time hysteresis) defined by (2.11) with  $\mu = 20$  or  $g(t) = 20 \exp(-20t)$ , and the nonlocal viscous damping defined by (2.12) with  $\mu = \infty$  or  $g(t) = \delta(t)$ . For each case there are taken four models: (model1) the exponential decay (2.9a), (model 2) the error function (2.9a), (model3) the hat (2.9b) and (model 4) the triangular shapes (2.9b). We take  $\alpha = 5$  and  $l_0 = 0.8$ . The number  $N$  of cnoidal functions is 4. For  $N > 4$  the increase in accuracy of results of the genetic algorithm is not significant.

The three roots of (4.3) are determined. These roots can have two distinct forms: (a) one root is real and the other two roots form a complex conjugate pair, or (b) all of the roots are real.

The complex conjugate pair of roots in case (a) corresponds to an underdamped oscillator that usually arises when the small damping assumption is made, while the real root corresponds to a purely dissipative motion. Case (b) represents an overdamped system which cannot sustain any oscillatory motion.



Table 5.1

The nonlocal viscoelastic damping: first five eigenvalues for a simply supported beam with one nonlocal viscoelastic damping patch

Model	Mode 1	Mode 2	Mode 3	Mode 4	Mode 5
1	$-4.74 \pm 20.15i$	$-0.26 \pm 71.42i$	$-0.045 \pm 160.98i$	$-0.017 \pm 287.31i$	$-0.0050 \pm 451.67i$
2	$-4.91 \pm 20.22i$	$-0.29 \pm 71.66i$	$-0.051 \pm 160.53i$	$-0.019 \pm 287.76i$	$-0.0051 \pm 451.71i$
3	$-4.75 \pm 20.16i$	$-0.23 \pm 71.09i$	$-0.038 \pm 160.51i$	$-0.013 \pm 287.98i$	$-0.0012 \pm 451.70i$
4	$-4.43 \pm 20.39i$	$-0.15 \pm 71.10i$	$-0.028 \pm 160.04i$	$-0.008 \pm 287.06i$	$-0.0011 \pm 451.74i$

Table 5.2

The nonlocal viscous damping: first five eigenvalues for a simply supported beam with one nonlocal viscous damping patch

Model	Mode 1	Mode 2	Mode 3	Mode 4	Mode 5
1	$-9.97 \pm 16.99i$	$-3.79 \pm 72.44i$	$-3.03 \pm 152.66i$	$-3.57 \pm 283.21i$	$-2.59 \pm 449.03i$
2	$-10.52 \pm 16.94i$	$-4.28 \pm 72.44i$	$-3.32 \pm 152.77i$	$-4.04 \pm 283.23i$	$-2.64 \pm 449.47i$
3	$-10.05 \pm 16.84i$	$-3.36 \pm 72.48i$	$-2.51 \pm 152.76i$	$-2.73 \pm 283.21i$	$-0.66 \pm 449.74i$
4	$-9.12 \pm 16.87i$	$-2.28 \pm 72.59i$	$-1.89 \pm 152.58i$	$-1.76 \pm 283.29i$	$-0.60 \pm 449.82i$

Table 5.1 shows the lower estimates for the first five eigenvalues for the beam with nonlocal viscoelastic damping. Table 5.2 shows the lower estimates of the first five eigenvalues for the second case of nonlocal viscous damping. It is observed that in both cases, the model 2 has the largest damping ratios for the first five eigenvalues, while model 4 has the smallest damping ratio. All damping models give for each mode, similar imaginary parts.

*Example 5.2.* Let us consider a simply supported aluminum beam of length  $L = 2$  m, with constant diameter  $d = 0.005$  m, the Young's modulus  $E = 70$  GPa and the mass density  $\rho = 2,700$  kg/m<sup>3</sup>, with two patches  $k = 2$  with  $x_1 = 0.2$ m and  $\Delta x_1 = 0.2$ m,  $x_2 = 1.6$ m and  $\Delta x_2 = 0.2$ m and thickness  $0.003$ m. We  $\alpha = 5$  and  $l_0 = 0.8$ . The table 5.3 shows the lower estimates of the first five eigenvalues for the beam with nonlocal viscoelastic damping.

Table 5.3

The nonlocal viscoelastic damping: first five eigenvalues for a simply supported beam with one nonlocal viscoelastic damping patch

Model	Mode 1	Mode 2	Mode 3	Mode 4	Mode 5
1	$-4.82 \pm 14.57i$	$-0.32 \pm 63.51i$	$-0.046 \pm 143.56i$	$-0.018 \pm 280.38i$	$-0.0052 \pm 413.33i$
2	$-4.90 \pm 14.99i$	$-0.39 \pm 63.60i$	$-0.053 \pm 143.63i$	$-0.019 \pm 280.42i$	$-0.0054 \pm 413.37i$
3	$-4.91 \pm 14.60i$	$-0.33 \pm 63.32i$	$-0.039 \pm 143.90i$	$-0.015 \pm 280.33i$	$-0.0013 \pm 413.11i$
4	$-4.65 \pm 13.86i$	$-0.27 \pm 63.19i$	$-0.029 \pm 143.42i$	$-0.009 \pm 280.25i$	$-0.0012 \pm 413.30i$

Table 5.4 shows the lower estimates of the first five eigenvalues for the beam for the nonlocal viscous damping. We see that the damping ratios for modes 1 and 2 are greater than those of example 5.1 for all cases and models. The next modes show increased values of the damping ratios, while the imaginary parts are

smaller than those of example 5.1. The model 2 has the largest damping ratios for the first five eigenvalues, while model 4 has the smallest damping ratio.

Table 5.4

The nonlocal viscous damping: first five eigenvalues for a simply supported beam with two nonlocal viscous damping patches

Model	Mode 1	Mode 2	Mode 3	Mode 4	Mode 5
1	$-10.07 \pm 15.09i$	$-3.99 \pm 70.54i$	$-3.05 \pm 142.46i$	$-3.58 \pm 270.06i$	$-2.60 \pm 423.03i$
2	$-10.76 \pm 15.22i$	$-4.77 \pm 70.55i$	$-3.39 \pm 142.45i$	$-4.07 \pm 270.00i$	$-2.65 \pm 423.22i$
3	$-10.35 \pm 15.13i$	$-3.66 \pm 70.68i$	$-2.57 \pm 142.77i$	$-2.75 \pm 270.12i$	$-0.67 \pm 423.31i$
4	$-9.40 \pm 15.53i$	$-2.58 \pm 70.68i$	$-1.91 \pm 142.78i$	$-1.77 \pm 270.04i$	$-0.65 \pm 423.30i$

*Example 5.3.* Let us consider a cantilever aluminum beam of length  $L = 2$  m, with variable diameter  $d_0 = 0.005$  m and  $a = 1$ , the Young's modulus  $E = 70$  GPa and the mass density  $\rho = 2,700$  kg/m<sup>3</sup>, with a single patch  $k = 1$  with  $x_1 = 0.2$  m and  $\Delta x_1 = 0.2$  m, and thickness 0.003 m. Table 5.5 shows the lower estimates of the first five eigenvalues for the cantilever beam with variable diameter and a nonlocal viscoelastic damping patch. Table 5.6 shows the lower estimates of the first five eigenvalues for the cantilever beam with variable diameter and a nonlocal viscous damping patch. As compared to results of the example 5.1, all damping ratios have increased for both cases. The imaginary parts also have increased. It is observed that the model 2 has the largest damping ratios for the first five eigenvalues, while model 4 has the smallest damping ratio.

Table 5.5

The nonlocal viscoelastic damping: first five eigenvalues for a cantiler beam with variable diameter and one nonlocal viscoelastic damping patch

Model	Mode 1	Mode 2	Mode 3	Mode 4	Mode 5
1	$-4.95 \pm 25.15i$	$-0.27 \pm 75.44i$	$-0.047 \pm 168.17i$	$-0.018 \pm 298.44i$	$-0.0051 \pm 466.29i$
2	$-5.02 \pm 25.35i$	$-0.31 \pm 75.63i$	$-0.053 \pm 168.33i$	$-0.019 \pm 298.84i$	$-0.0053 \pm 466.37i$
3	$-4.95 \pm 25.52i$	$-0.25 \pm 75.32i$	$-0.040 \pm 168.23i$	$-0.014 \pm 298.58i$	$-0.0013 \pm 466.47i$
4	$-4.65 \pm 24.77i$	$-0.16 \pm 75.10i$	$-0.031 \pm 168.39i$	$-0.009 \pm 298.33i$	$-0.0012 \pm 466.51i$

Table 5.6

The nonlocal viscous damping: first five eigenvalues for a cantiler beam with variable diameter and one nonlocal viscous damping patch

Model	Mode 1	Mode 2	Mode 3	Mode 4	Mode 5
1	$-10.42 \pm 17.64i$	$-3.81 \pm 74.60i$	$-3.18 \pm 166.96i$	$-3.72 \pm 298.71i$	$-2.66 \pm 467.03i$
2	$-10.97 \pm 17.69i$	$-4.30 \pm 74.54i$	$-3.47 \pm 167.17i$	$-4.19 \pm 299.01i$	$-2.72 \pm 467.00i$
3	$-10.51 \pm 17.59i$	$-3.38 \pm 74.64i$	$-2.66 \pm 167.39i$	$-2.88 \pm 299.02i$	$-0.74 \pm 467.24i$
4	$-9.56 \pm 18.18i$	$-2.31 \pm 74.75i$	$-2.04 \pm 167.08i$	$-1.92 \pm 298.79i$	$-0.50 \pm 467.12i$

## 6. THE INVERSE APPROACH AND RESULTS

In the formulation of the inverse problem, the bound optimization formulation of Bendsoe, Olhoff and Taylor [22] and Pedersen [2] is used. The unknown parameters are the coordinates  $x_j$  and the lengths of patches  $\Delta x_j$ ,  $j=1,2,\dots,k_p$ , under the conditions  $x_2 \geq x_1 + \Delta x_1$ ,  $x_i \geq x_{i-1} + \Delta x_{i-1}$ ,  $i=2,\dots,k_p$ . We suppose that the number  $k_p$  of patches is prescribed.

The inverse problem consists in determination of  $x_j$ ,  $\Delta x_j$ ,  $j=1,2,\dots,k_p$ , so that all eigenvalues to stay above a given complex constant  $C_1 + iC_2$ . The formulation of the optimization problem is

Determine  $x_j$ ,  $\Delta x_j$ ,  $j=1,2,\dots,k_p$ , from:

$$\begin{aligned} & \text{maximize } |C_1|, |C_2| \\ & \text{subject to : all } \operatorname{Re}|\omega| \geq |C_1|, \operatorname{Im}|\omega| \geq |C_2| \\ & \sum_{j=1}^N (P_j + \rho\omega^2 Q_j + \omega R_j + Y_j) = 0, \\ & Y_j = 2\omega A_j \sum_{i=1}^k \int_{x_i}^{x_i + \Delta x_i} \int_{-\infty}^t C(x, \xi, t - \tau) (\operatorname{cn}\eta_j \operatorname{sn}\eta_j \operatorname{dn}\eta_j) d\tau d\xi, \\ & \eta_j = \eta |m_j = k\xi - \omega\tau + \varphi. \end{aligned} \quad (6.1)$$

where  $P, Q, R$  are polynomials in  $\operatorname{cn}$ ,  $\operatorname{sn}$  and  $\operatorname{dn}$ .

If we want to maximize the difference between two consecutive eigenvalues, say  $\omega_i$  and  $\omega_{i+1}$ , the problem can be formulated as

Determine  $x_j$ ,  $\Delta x_j$ ,  $j=1,2,\dots,k_p$ , from:

$$\begin{aligned} & \text{maximize } \operatorname{Re}|C_4 - C_3|, \operatorname{Im}|C_4 - C_3| \\ & \text{subject to : } \operatorname{Re}|\omega_i| \geq \operatorname{Re}|C_2|, \operatorname{Re}|\omega_{i+1}| \geq \operatorname{Re}|C_3|, \\ & \operatorname{Im}|\omega_i| \geq \operatorname{Im}|C_2|, \operatorname{Im}|\omega_{i+1}| \geq \operatorname{Im}|C_3| \\ & \sum_{j=1}^N (P_j + \rho\omega^2 Q_j + \omega R_j + Y_j) = 0, \\ & Y_j = 2\omega A_j \sum_{i=1}^k \int_{x_i}^{x_i + \Delta x_i} \int_{-\infty}^t C(x, \xi, t - \tau) (\operatorname{cn}\eta_j \operatorname{sn}\eta_j \operatorname{dn}\eta_j) d\tau d\xi, \\ & \eta_j = \eta |m_j = k\xi - \omega\tau + \varphi. \end{aligned} \quad (6.2)$$

*Example 6.1.* Let us consider the example 5.1. of a simply supported aluminum beam of length  $L=2$  m, with constant diameter  $d=0.005$  m, the Young's modulus  $E=70$  GPa and the mass density  $\rho=2,700$  kg/m<sup>3</sup>, with a single

patch  $k=1$ , of unknown  $x_1$  [m], the given length  $\Delta x_1 = 0.2$  m, and thickness  $h_p = 0.003$  m. Both cases of nonlocal viscoelastic damping ( $\mu = 20$ ), and of nonlocal viscous damping ( $\mu = \infty$ ) are treated. For each case there is taken the model 1 with  $\alpha = 5$  and  $l_0 = 0.8$ . The number  $N$  of cnoidal functions is 4. The inverse problem (6.1) with  $C_1 + iC_2 = -0.0050 \pm 451.67i$  for the case 1, and  $C_1 + iC_2 = -2.59 \pm 449.03i$  for the second case is solved by using a genetic algorithm. The run-time parameters of genetic algorithm are: population size 120, number of generations 60, overall crossover probability 0.9, mutation probability 0.03. The number of iteration for the first case is 496, and for the second case 388.

Table 6.1

Case 1: the location of the viscoelastic damping patch (model 1) and the first five eigenvalues for a simply supported beam

	Mode 1	Mode 2	Mode 3	Mode 4	Mode 5
	$-5.87 \pm 744.55i$	$-4.96 \pm 1493.49i$	$-3.24 \pm 1873.57i$	$-2.77 \pm 2637.39i$	$-0.52 \pm 3553.46i$
$x_1$	1	1	0.46 and 1.34	0.31 and 1.49	0.22 and 1.58

Table 6.2

Case 2: the location of the nonlocal viscous damping patch (model 1) and the first five eigenvalues for a simply supported beam

	Mode 1	Mode 2	Mode 3	Mode 4	Mode 5
1	$-11.22 \pm 715.1i$	$-6.29 \pm 1272.47i$	$-5.01 \pm 1622.66i$	$-4.37 \pm 2290.11i$	$-3.99 \pm 3353.33i$
$x_1$	1	1	0.19 and 1.61	0.33 and 1.47	0.12 and 1.68

Table 6.1 gives the estimates for  $x_1$  and the first five eigenvalues of the beam in the first case of nonlocal viscoelastic damping. Table 6.2 gives the estimates for  $x_1$  and the first five eigenvalues in the second case of nonlocal viscous damping. In both cases, it is maintained the same patch length  $\Delta x_1$ . Modes 3-5 have two estimates for  $x_1$ , symmetrically with respect to the ends of beam. By comparing to the similar example 5.1, the damping ratios of all modes are significantly increased. The imaginary parts are greater than those of example 5.1. In addition, all eigenvalues stay above a given complex constant  $C_1 + iC_2$ .

## 7. SUMMARY AND CONCLUSIONS

In this paper, the bending of Euler-Bernoulli beams with external nonlocal damping patches is studied. The nonlocal damping force is modeled as a weighted average of the velocity field over the spatial domain, determined by a kernel function based on distance measures.

The following three case studies are analyzed for the nonlocal viscoelastic

damping (or time hysteresis) defined by (2.11) with  $\mu = 20$  or  $g(t) = 20\exp(-20t)$ , and for the nonlocal viscous damping defined by (2.12) with  $\mu = \infty$  or  $g(t) = \delta(t)$ . For each case there are taken four models: (model1) the exponential decay (2.9a), (model2) the error function (2.9a), (model3) the hat (2.9b) and (model 4) the triangular shapes (2.9b);

(1) a simply supported aluminum beam with a single nonlocal damping patch;

(2) a simply supported aluminum beam with two nonlocal damping patches;

(3) a cantilever aluminum beam with variable with a single nonlocal damping patch.

The lower estimates for the first five eigenvalues are given. In all cases, the model 2 has the largest damping ratios for the first five eigenvalues, while model 4 has the smallest damping ratio.

The performance with respect to eigenvalues is discussed next in order to avoid resonance. The optimization is performed by determining the location of patches from maximizing eigenvalues or gap between them. The formulation of the optimization problem (6.1) of maximizing eigenvalues is implemented on the example of a simply supported aluminum beam with a single patch of unknown location  $x_1$  and given length  $\Delta x_1$ . The location  $x_1$  is determined and also the first five eigenvalues of the beam in the first case of nonlocal viscoelastic damping and in the second case of nonlocal viscous damping. In both cases, it is maintained the same patch length  $\Delta x_1$ . Modes 3-5 have two estimates for  $x_1$ , symmetrically with respect to the ends of beam. By comparing to the similar above example (1), the damping ratios of all modes are significantly increased. The imaginary parts are greater than those of example 5.1. In addition, all eigenvalues stay above a given complex constant.

**Acknowledgements.** Supports for this work by the CEEX postdoctoral grant 1531/2006 and the CNCSIS grant 55/2007 code 160/2005 are gratefully acknowledged.

*Received on May 9, 2008.*

#### REFERENCES

1. Abrete, S., *Optimal design of laminated plates and shells*, Composite structures, **29**, pp. 269-286, 1994.
2. Pedersen, N.L., *On simultaneous shape and orientational design for eigenfrequency optimisation*, Danish Center for Applied Mathematics and Mechanics, report nr. 714, June 2006.
3. Pedersen, N.L., *Designing plates for minimum internal resonance*, Struct. Multidisc. Optim., **28**, 1, pp. 1-10, 2004.
4. Pedersen, N.L., *Optimization of holes in plates for control of eigenfrequencies*, Struct. Multidisc. Optim., **30**, 4, pp. 297-307, 2005.
5. Eringen, A.C., Edelen, D.G.B., *Nonlocal elasticity*, International Journal of Engineering Science, **10**, 3, pp. 233-248, 1972.
6. Polizzotto, C., *Non-local elasticity and related variational principles*, International Journal of Solids and Structures, **38** (42-43), pp. 7359-7380, 2001.

7. Ahmadi, G., *Linear theory of nonlocal viscoelasticity*, International Journal of Non-Linear Mechanics, **10**, 2, pp. 253-258, 1975.
8. Nowinski, J.L., *On the non-local aspects of stress in a viscoelastic medium*, International Journal of Non-Linear Mechanics, **21**, 6, pp. 439-446, 1986.
9. Russell, D.L., *On mathematical models for the elastic beam with frequency-proportional damping*, In: Banks, H.T. (Ed.), *Control and Estimation in Distributed Parameter Systems*, SIAM, Philadelphia, PA, pp. 125-169, 1992.
10. Ghoneim, H., *Fluid surface damping versus constrained layer damping for vibration suppression of simply supported beams*, Smart Materials and Structures, **6**, 1, pp. 40-46, 1997.
11. Lei, Y., Friswell, M.I., Adhikari, S., *A Galerkin method for distributed systems with nonlocal damping*, International Journal of Solids and Structures, **43**, pp. 3381-3400, 2006.
12. Banks, H.T., Inman, D.J., *On damping mechanisms in beams*, Journal of Applied Mechanics, **58**, 3, 716-723, 1991.
13. Banks, H.T., Wang, Y., Inman, D.J., *Bending and shear damping in beams—frequency-domain estimation techniques*, Journal of Vibration and Acoustics, **116**, 2, pp. 188-197, 1994.
14. Sorrentino, S., Marchesiello, S., Piombo, B.A.D., *A new analytical technique for vibration analysis of non-proportionally damped beams*, Journal of Sound and Vibration **265**, 4, pp. 765-782, 2003.
15. Baldovin, D., Delsanto, P.P., Mitu, A.M., Chiroiu, V., *On the modal strain energy approach*, Annual Symposium of the Institute of Solid Mechanics SISOM2007, may 2007.
16. Munteanu, L., Donescu, St., *Introduction to Soliton Theory: Applications to Mechanics*, Book Series "Fundamental Theories of Physics", **143**, Kluwer Academic Publishers, 2004.
17. Chiroiu, V., Chiroiu, C., *Probleme inverse în mecanică* (Inverse problems in mechanics), Edit. Academiei, 2003.
18. Osborne, A. R., *Soliton physics and the periodic inverse scattering transform*, Physica D, **86**, pp. 81-89, 1995.
19. Abramowitz, M. and Stegun, I. A. (eds.), *Handbook of mathematical functions*, U. S. Dept. of Commerce, 1984.
20. Bendsoe, M.P., Olhoff, N., Taylor, J.E., *A variational formulation for multicriteria structural optimization*, Journal of Structural Mechanics, **11**, 4, pp. 523-544, 1983.